

## Orientation and alignment of collisionally excited atomic states

C. D. Lin and R. Shingal

*Department of Physics, Kansas State University, Manhattan, Kansas 66506*

A. Jain

*Department of Physics, Florida A&M University, Tallahassee, Florida 32307*

W. Fritsch

*Bereich Physik, Hahn-Meitner Institute, Berlin D-1000, Berlin 39, West Germany*

(Received 9 January 1989)

The orientation and alignment parameters of atomic excited states of hydrogen and helium atoms formed in collisions with electrons, positrons, protons, and antiprotons are examined. For the orientation parameter  $\langle L_y \rangle$  (defined to be the expectation value of the electronic angular momentum perpendicular to the collision plane), it is found that the signs of  $\langle L_y \rangle$  for proton and positron impact are negative, consistent with the prediction of the classical model with a repulsive force. For electron and antiproton impact, except for electron scattering at large angles, the signs of  $\langle L_y \rangle$  are positive, consistent with the classical model with an attractive force. A simple semiempirical scaling of  $\langle L_y \rangle$  for electron-impact excitations to  $2p$  states was found. The orientation of  $2p$  states formed in electron capture in proton-hydrogen-atom collisions and in positron-hydrogen-atom collisions are also studied and the angular dependences of  $\langle L_y \rangle$  are found to show similar behavior. We also examine the orientation parameters for excitation and capture to  $3d$  states and the alignment angles for excitation and capture to  $2p$  states. It is found that in the latter cases these parameters do not show similar simple dependences with scattering angles.

### I. INTRODUCTION

The study of polarization and/or angular distribution of atomic radiation emitted after impact excitation in coincidence with scattered particles has yielded a wealth of detailed information on the mechanism and dynamics of collisional excitation of atoms by charged particles. From these measurements the scattering amplitudes of the magnetic substates of the excited atoms can be extracted in the form of orientation and alignment parameters. The alignment parameters characterize the anisotropic charge cloud distribution while the orientation parameter describes the rotation of the atomic excited states,<sup>1-3</sup> and provide complementary information on the formation of excited states not available from measurements of cross sections alone.

Since the early 1970s there has been a great deal of experimental effort in the determination of orientation and alignment parameters of simple atoms by electron impact, and to a less extent by atom and ion impact. Despite the continuing efforts, only a limited number of collision systems have been investigated. On the theoretical side, these parameters have been extracted from a number of calculations and compared with experiments. A compilation of all the data prior to 1986 from different experimental groups, as well as their evaluations, has been completed recently by Andersen *et al.*<sup>4</sup> In this article, results from different theoretical models have also been discussed.

Results from these earlier studies showed that the orientation parameter displayed intriguing features. The

orientation parameter is defined as the expectation value of the electronic angular momentum perpendicular to the scattering plane  $\langle \phi | L_y | \phi \rangle = \langle L_y \rangle$  for the excited state  $\phi$ . (For simplicity we will use  $L_y$  to denote the expectation value  $\langle L_y \rangle$  when there is no danger of confusion.) We have assumed that the  $xz$  plane is the collision plane and the  $y$  axis is perpendicular to it. If the orientation of the initial state is zero, then classically this quantity also corresponds to the angular momentum transferred to the electron by the projectile in the collision. According to the first-order Born approximation for direct excitation processes, the orientation parameter is universally zero at all scattering angles. This means that there is no net angular momentum transferred to the electron. Experimentally, for electron-impact excitation of helium to  $2^1P$  states, it has been observed that  $L_y$  increases monotonically from zero at small angles to a maximum, and then decreases monotonically at large scattering angles, reaching negative values before it approaches zero again at the backward scattering angle<sup>4</sup> (see Fig. 1). The fact that  $L_y$  vanishes at  $\theta=0^\circ$  and  $180^\circ$  is understood classically since there is no torque exerted to the atom by the projectile in these two limits. On the other hand, the variation of  $L_y$  with respect to scattering angles is not easily understood. It has been found that the shape of  $\langle L_y \rangle$  is quite universal at different collision energies: only the positions where  $L_y$  is maximum and where  $L_y$  vanishes are shifted. This simple behavior prompts attempts to interpret the results in terms of simple models.

Theoretically, it has been shown that the distorted-wave Born approximation<sup>5</sup> (DWBA), as well as the

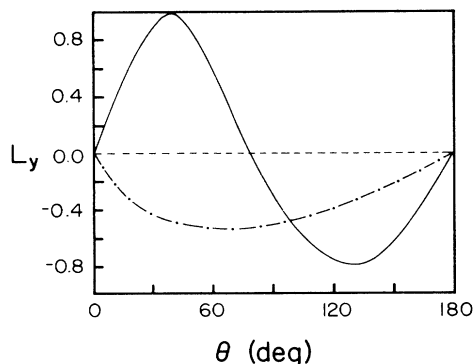


FIG. 1. Typical angular dependence of  $\langle L_y \rangle$  as a function of scattering angles for electron-impact (solid line) and positron-impact (dash-dotted lines) excitations to helium  $2^1P$  states or to hydrogenic  $2p$  states.

many-body perturbation theory<sup>6</sup> (which is similar to the DWBA in essence), are capable of predicting the observed dependence of  $L_y$  on the scattering angles and the collision energies. Despite such good agreement, there remain many questions. First, it is surprising that the DWBA is capable of predicting accurately the measured  $L_y$  when the first Born approximation fails completely. What is the basic factor included in the DWBA which is responsible for predicting the observed behavior of  $L_y$ ? Second, the simple near-universal behavior of  $L_y$  does not come out obviously from the DWBA or other calculations. In fact, it appears that  $L_y$  is relatively sensitive to the potentials chosen in the DWBA calculations. Third, the intuitive classical model,<sup>7</sup> despite its lack of solid theoretical basis,<sup>8</sup> is still very appealing in explaining the observed  $L_y$ . According to this model where the projectile electron is treated classically, the positive  $L_y$  at small scattering angles was due to the effective attractive force between the incident electron and the atom at glancing collisions, while the negative  $L_y$  was due to the effective repulsive force when the incident electron penetrates deep inside the atom. In the other words, the effective trajectories were used to interpret the observed angular dependences of  $L_y$ . The basic assumptions of this model for electron-impact excitation of atoms have been refuted<sup>9</sup> since the effective interaction between an electron and an atom is *always* attractive. However, the prediction of the classical model is not completely erroneous. For positron-impact excitation of atoms, the DWBA calculation shows that  $L_y$  is always negative at all scattering angles. The effective interaction between a positron and an atom is always repulsive and thus the calculated  $L_y$  is consistent with the classical model. Thus the question remains whether the sign of  $L_y$  has anything to do with the effective attractive or repulsive interactions in general.

To understand the role of effective interactions or the trajectories on the sign of  $L_y$ , it is more practical to examine the situation for heavy-particle collisions where the concept of classical trajectories is applicable. Unfor-

tunately, there are very little experimental data for such studies in heavy-particle collisions, particularly in the energy region where the collision velocities are comparable to those in electron-impact excitations. At such velocities the collision energies are in the tens of keV/amu and the heavy projectiles are scattered mostly in the forward directions, thus making coincidence measurements extremely difficult. For heavy-particle collisions at lower energies where a number of experiments have been carried out, the role of the formation of quasimolecules becomes important and a different collision mechanism applies. It is then difficult to compare these results with data from electron scattering.

The goal of this paper is to address the dependence of the orientation parameter on the charge, or more precisely, the effective interaction potential between the projectiles and simple target atoms. In particular, calculations from the literature for hydrogen and helium targets by electron and by positron impacts are reevaluated; they are then compared with calculations that we have carried out for collisions involving heavy ions. In this article, we limit the projectiles to protons and antiprotons only. The collision velocities are limited to the range of 1–2.5 a.u. and the results from electron, positron, proton, and antiproton impacts are analyzed. We are searching for general trends and similarities in the calculated  $L_y$  in order to assess the possibility of simple models for interpreting the variation of the sign of the orientation parameter for different projectiles. We remark that for projectiles with positive charges, electron-transfer channels should be considered as well.

The rest of this paper is organized as follows. In Sec. II we first summarize the basic equations relating the scattering amplitudes to the orientation and alignment parameters. We then review theoretical models used in the calculation of these parameters for electron, positron, and heavy-particle collisions with atoms. In Sec. III A we review results from electron and positron impacts, taking data from the literature. In III B we address the scaling relation for  $L_y$ . In III C we show the calculated  $L_y$  for excitation to  $2^1P$  and  $3^1P$  in proton-helium and antiproton-helium collisions using a one-center atomic-orbital expansion where the electron-transfer channels were neglected. We will show that the “propensity rule” is applicable to such collisions. We will also discuss the role of effective interactions on the sign of  $L_y$ . In III D we discuss proton-hydrogen collisions where the  $\langle L_y \rangle$  for excitation and charge transfer to  $2p$  states are examined. We will also compare the orientation of  $2p$  states in the positronium formation (in III E) in positron-hydrogen-atom scattering with that in proton-hydrogen-atom scattering. In III F we discuss the  $L_y$  for the  $3d$  states formed in direct excitation as well as in charge-transfer channels.

The orientation parameter is only one of the state multipoles that can be constructed out of the full density matrix. A complete characterization of the collisionally excited states requires the specification of other parameters.<sup>9–12</sup> Different sets of such parameters have been introduced in the literature but we will not examine them here except for a brief summary on the alignment angle

in Sec. IV. Conclusions and a summary are given in Sec. V.

## II. THEORETICAL METHODS

In this section we first summarize the definition of orientation and alignment parameters in terms of scattering amplitudes. We then describe the theoretical models used in the calculation of transition amplitudes. We will consider inelastic processes from the initial  $1s$  state only. The target atoms are either hydrogen atom or helium atom; the projectiles are electrons, positrons, protons, or antiprotons. We emphasize that for a hydrogen-atom target, the role of the electron spin is neglected in our discussion.

### A. Orientation and alignment parameters for $np$ states

To describe the orientation and alignment of an excited atom, we need to specify the quantization axis and the coordinate frame. The directions of the incident vector  $\mathbf{k}_i$  and the scattered wave vector  $\mathbf{k}_f$  define the scattering plane. In the collision frame the collision plane is chosen to be the  $xz$  plane, with the  $z$  axis being along  $\mathbf{k}_i$ , and the positive  $x$  axis is defined such that  $\mathbf{k}_f$  points into the first or second quadrants of the  $xz$  plane. The  $y$  axis is normal to the scattering plane such that  $x, y,$  and  $z$  axes follow the right-hand rule. Let us consider the collisionally excited  $2p$  states which can be represented by the wave function,

$$\begin{aligned}\psi &= a_{2p_0} \phi_{2p_0} + a_{2p_1} \phi_{2p_1} + a_{2p_{-1}} \phi_{2p_{-1}} \\ &= a_0 \phi_0 + a_1 \phi_1 + a_{-1} \phi_{-1},\end{aligned}\quad (1)$$

where the second relation defines the abbreviated notation. In (1) above, the subscript to  $2p$  refers to the magnetic quantum number, the  $a$ 's are the transition amplitudes to each state, and the  $\phi$ 's are the  $2p$  wave functions. Since the initial  $s$  state has even reflection symmetry with respect to the scattering plane and the interaction Hamiltonian has reflection symmetry, the amplitudes  $a_{-1} = -a_1$ . Notice that the quantization axis for the magnetic quantum numbers refers to the direction of the incident beam. This collision frame is the coordinate system used frequently in theoretical calculations.

One can also define a natural frame  $x', y',$  and  $z'$  where  $z' = y, x' = z,$  and  $y' = x$ . The same wave function in (1) with respect to the natural frame is

$$\psi = a'_0 \phi'_0 + a'_1 \phi'_1 + a'_{-1} \phi'_{-1}, \quad (2)$$

where the quantization axis is now referred to the  $z' = y$  axis ( $a'_0 \equiv 0$  since it is associated with a state which is odd with respect to the  $x'y'$  plane). With respect to this natural frame, the orientation parameter is now given by

$$\langle L_y \rangle = \langle L_{z'} \rangle = |a'_1|^2 - |a'_{-1}|^2, \quad (3)$$

where

$$\begin{aligned}a'_1 &= -a_0/\sqrt{2} - ia_1, \\ a'_{-1} &= a_0/\sqrt{2} - ia_1.\end{aligned}\quad (4)$$

With respect to the natural frame, the orientation parameter is simply the difference in the probabilities for populating  $m' = +1$  and  $m' = -1$  states. This is the quantity on which we will focus primarily in this article. For convenience we will normalize the total excitation probabilities to  $2p$  states to one, i.e., we normalize  $a_0$  and  $a_1$  such that

$$|a_0|^2 + 2|a_1|^2 = 1. \quad (5)$$

To completely describe the scattering amplitudes of  $2p$  states we have to specify two complex amplitudes. Since the absolute phase is not important, there are three real parameters to be determined. If the scattering amplitudes are normalized as in (5), then only two real parameters are to be determined. These two parameters were chosen to be the  $\lambda$  and  $\chi$  parameters by Eminyan *et al.*<sup>13,14</sup> where

$$\lambda = |a_0|^2 / (|a_0|^2 + 2|a_1|^2) \quad (6a)$$

and

$$\chi = \arg(a_1/a_0). \quad (6b)$$

In other words, the  $\lambda$  gives the fractional probability for excitation to the  $2p_0$  state, while  $\chi$  gives the relative phase between the  $2p_1$  and  $2p_0$  amplitudes. The parameters  $\lambda$  and  $\chi$  can be determined by measuring the polarization of the Lyman radiation from the decay of  $2p$  states or from the angular distribution of the photons emitted. To determine the sign of  $\sin\chi$  uniquely, circular polarization of the Lyman radiation has to be measured.

An alternative set of parameters has been proposed by Andersen *et al.*<sup>4</sup> Instead of  $\lambda$  and  $\chi$ , they suggested that the orientation parameter  $\langle L_y \rangle$  and an alignment angle  $\gamma$  are to be used since these two parameters can be related to the wave function of the excited  $2p$  states directly. The orientation  $\langle L_y \rangle$ , as discussed earlier, describes the rotation of the electronic cloud, while the angle  $\gamma$  is the angle between the major axis of the electron cloud on the collision plane with respect to the incident direction, i.e., the alignment of the electron cloud. These two sets of parameters are related by

$$\langle L_y \rangle = -2[\lambda(1-\lambda)]^{1/2} \sin\chi, \quad (7a)$$

$$\tan 2\gamma = \frac{2[\lambda(1-\lambda)]^{1/2}}{1-2\lambda} \cos\chi. \quad (7b)$$

These two parameters have been adopted by Andersen *et al.*<sup>4</sup> for the characterization of the excited  $2p$  states. The other advantage of the orientation and alignment parameters in describing excited  $2p$  states is that they can be related to classical quantities and thus a classical interpretation of experimental results may be possible. It is to be noted that these same parameters can be used to describe  $np$  ( $n > 2$ ) states as well.

### B. The orientation parameter for $3d$ states

The coherence between the  $3d$  magnetic substates excited from an initial  $s$  state is described by five real pa-

rameters. Experimental and theoretical studies of the coherence of  $3d$  (and  $nd$ ) states are quite scarce. In this paper we will address only the  $\langle L_y \rangle$  parameter. In terms of the scattering amplitudes in the collision frame and in the natural frame, we have

$$\langle L_y \rangle = 4 \operatorname{Im}(\sqrt{3}/2 a_{3d_0} a_{3d_1}^* + a_{3d_1} a_{3d_2}^*), \quad (8a)$$

$$= 2|a'_{3d_2}|^2 - 2|a'_{3d_{-2}}|^2, \quad (8b)$$

where in the natural frame (the primed amplitudes) the  $m'=1$  and  $-1$  states are not populated because these states have odd symmetry with respect to the scattering plane. The relations between the amplitudes in the two frames are<sup>15</sup>

$$a'_0 = -\frac{1}{2}a_0 - \sqrt{3}/2a_2, \quad (9a)$$

$$a'_{\pm 2} = \sqrt{3}/8a_0 \pm ia_1 - \frac{1}{2}a_2. \quad (9b)$$

It is to be noted that the amplitudes are normalized so that the total probability to  $3d$  states is unity.

### C. Scattering calculations

From the theoretical viewpoint, all information about orientation and other parameters is contained in the scattering amplitudes. In the intermediate-energy region where the angular dependence of the orientation parameter is simple, the theoretical models used for describing the electron- and positron-impact excitations of helium or hydrogen atoms are the distorted-wave Born approximation of Madison and Winters,<sup>5</sup> the first-order many-body perturbation theory of Cartwright and Csanak,<sup>6</sup> the close coupling method of Fon *et al.*,<sup>16</sup> and the multichannel eikonal theory of Mansky and Flannery.<sup>17</sup> We will not discuss these models here except to quote some of their results.

For heavy-particle collisions, we employed two models. In describing collisions between antiprotons with helium and proton-helium collisions at high energies, we used the one-center atomic-orbital expansion method. The time-dependent wave function  $\psi(\mathbf{r}, t)$  of the electron satisfies

$$(H - i\partial/\partial t)\psi = 0, \quad (10a)$$

where the Hamiltonian

$$H = -\frac{1}{2}\nabla^2 - \frac{Z_p}{r_p} + V(r_t). \quad (10b)$$

Atomic units are used. In (10b),  $Z_p$  is the charge of the projectile, and the target atom is described by a model potential  $V(r)$ . In the one-center atomic-orbital expansion method the electronic wave functions are expanded in terms of target eigenstates

$$\psi(\mathbf{r}, t) = \sum_i a_i(t) \phi_i(\mathbf{r}) \exp(-i\varepsilon_i t), \quad (11)$$

where  $\phi_i$ 's are the target eigenstates with eigenenergies  $\varepsilon_i$  and the coordinates are referred to the target center. Substitution of (11) into (10a) gives a set of first-order coupled differential equations for  $a_i(t)$  which can be

solved to give scattering amplitudes at  $t \rightarrow +\infty$ . The size of the basis set used will be discussed when the results are presented.

For collisions at lower energies between protons and hydrogen atoms, we used a two-center atomic-orbital expansion method.<sup>18-20</sup> The time-dependent wave function is expanded in terms of the eigenstates of both the target and the projectile atoms,

$$\psi(\mathbf{r}, t) = \sum_i a_i(t) \phi_i(\mathbf{r}_t, t) + \sum_j b_j(t) \phi_j(\mathbf{r}_p, t), \quad (12)$$

where the basis functions on the target and on the projectile centers have been included. The base functions above include electron translational factors. Substitution of (12) into (10) gives a set of coupled first-order equations for the coefficients  $a_i(t)$  and  $b_j(t)$  from which excitation and charge-transfer amplitudes can be obtained. These amplitudes are then used to calculate the orientation and other parameters. Details of these calculations are given elsewhere.<sup>19-22</sup> We just point out that these methods have been shown to give accurate total excitation and electron capture cross sections for many systems<sup>22</sup> in the intermediate-energy region.

## III. THE ORIENTATION PARAMETER

In this section we first summarize in III A results of measurements and calculations of the orientation parameter  $L_y$  for electron-impact excitation of simple systems such as hydrogen and helium atoms. We stress the near-universal behavior of  $L_y$  as a function of scattering angles. We will then show in III B that there is a simple scaling relation if one introduces an equivalent impact parameter for each scattering angle. In III C we present the orientation parameters of the excitation of helium by proton and by antiproton impact. The results are then compared with those obtained from the electron and positron impact. In III D we examine the orientation for proton collisions with hydrogen atoms where the orientations of the  $2p$  states in both the charge transfer and the excitation channels are investigated simultaneously. Our major goal is to see if the  $L_y$  parameter displays any general behavior as the collision energies are varied. We also compare in III E the orientation of the positronium  $2p$  states in positron-hydrogen collisions obtained in the distorted-wave calculation. In III F we examine the orientation parameter for the  $3d$  states formed either by direct excitation or by electron capture.

### A. Orientation of $2p$ states by electron and positron impact

Most of the experiments to date on the orientation of excited states have been carried out by electron impact (see the compilation of Andersen *et al.*<sup>4</sup>). Although there is no experimental  $L_y$  data from positron-atom excitations, we include theoretical results in the following general discussion.

(1) The orientation parameters for electron- and positron-impact excitation to  $2p$  states versus scattering angles are typically represented by Fig. 1. For electron

impact,  $L_y$  is positive at small angles and negative at large angles. The angle  $\theta_0$  where  $L_y$  vanishes becomes smaller at increasing scattering energies. Such angular dependence of  $L_y$  has been found experimentally for electron impact on helium to  $2^1P$ , to  $3^1P$ , and to  $2^3P$  over a certain angular range, and theoretically for electron excitation of helium to  $n^1P$  and to  $n^3P$  ( $n=3-8$ ), by electron-impact excitation of hydrogen atoms to  $2p$  and electron-impact excitation of hydrogenic ions<sup>20</sup> to  $2p$  (neglecting the spin of the electrons) theoretically (a complete reference to these data can be found in Sec. 3 of Ref. 4). Since theoretical calculations such as the DWBA and the first-order many-body perturbation theory are in good qualitative agreement with experimental results when comparison is possible, we rely on some of the theoretical results for the analysis here. In fact, we will adopt the recommended  $L_y$  by Andersen *et al.* for electron-impact data in the analysis below. For positron-impact excitation, theoretical results indicate that  $L_y$  is always negative at all angles and all energies.

(2) The near-universal results discussed above make it very attractive for searching simple physical models for  $L_y$ . According to the classical model, if the force between the incident particle and the target is attractive, the angular momentum of the target atom will increase after the collision. Similarly, if it is a repulsive force, the angular momentum of the target will decrease. Since the initial angular momentum is zero, the change of the target angular momentum is the angular momentum of the target  $L_y$  after the collision. Therefore this model would explain the observed angular dependence of  $L_y$  if the effective interaction between the incident electron and the target atom is attractive at small scattering angles and repulsive at large scattering angles. Such attractive interactions were attributed<sup>7</sup> to the polarization potentials for glancing collisions (small scattering angles), and the repulsive interactions were attributed to the Coulomb repulsion between the incident electron and the target electrons for close collisions (large scattering angles). The theoretical basis for this model, however, is not well founded. The effective interaction between an electron and a neutral atom is always attractive and the polarization potential has no effect on the calculated  $L_y$ .<sup>8</sup> Recognizing this fact we note that the classical model can only "explain" the positive  $L_y$  part. The negative  $L_y$  part was interpreted quantum mechanically by Madison *et al.*<sup>8</sup> as due to the strong attractive potential which results in large phase shifts and the interference among the partial waves (this interpretation would not affect the positron-impact results since the effective interaction is repulsive in this case and the phase shifts are negative). In other words, there is no simple classical interpretation for the negative  $L_y$  for electron-impact excitations.

(3) Theoretical calculations for positron-impact excitation to  $2p$  states indicate that  $L_y$  is always negative. One notes that the effective interaction between a positron and an atom is always repulsive and according to the classical model, one would expect a negative  $L_y$ , in consistency with the calculated results. Thus the question rises again: Can one correlate the sign of  $L_y$  to the

effective interactions?

(4) Although the negative  $L_y$  at large angles for electron impact cannot be explained by the classical model, it is not inconsistent with a quantum interpretation by attributing it to the trajectory effects or to the effective interactions between the projectile and the target atom. One clue to such a relation is that the DWBA appears to work quite well in interpreting the measured  $L_y$  while the plane wave Born approximation (PWBA) gives completely wrong results. The major difference between the DWBA and PWBA is the effective interaction potential included in the DWBA. In this respect, one can speculate that the negative  $L_y$  results from the large accumulated phase difference in the scattering amplitudes as the incident electron penetrates deep inside the atom. Such phases cannot be obtained in classical theories. It is further noted that exchange interaction is not responsible for the negative  $L_y$  at large angles since calculations with and without inclusion of exchange effect give similar results.<sup>21</sup>

Another clue which tempts us to examine the trajectory effects further is the apparent scaling relations of  $L_y$ . This is addressed separately in Sec. III B.

#### B. Scaling relations for $L_y$ in electron-impact excitations

The energy dependence of  $L_y$  appears to display some simple scaling relation. If we assume that the interaction between the electron and the target atom is governed by the Coulomb interaction, there is a one-to-one correspondence between the scattering angle  $\theta$  and the impact parameter  $b$ ,

$$b = \frac{Z}{2E} \cot(\theta/2), \quad (13)$$

where the scattering energy  $E$  and impact parameter  $b$  are given in atomic units. In Table I we display three special angles for each energy  $E$ : (1)  $\theta_0$ , defined as the angle where  $L_y$  vanishes; (2)  $\theta_{\max}$ , the angle where  $L_y$  is maximum; and (3)  $\theta_{\min}$ , the angle where  $L_y$  is minimum.

TABLE I. Scattering angles  $\theta_{\max}$ ,  $\theta_{\min}$ , and  $\theta_0$  where  $\langle L_y \rangle$  has maximum, minimum, and zero values, respectively, versus the electron scattering energies for electron-impact excitations to He( $2^1P$ ) states. We list two sets of angles for  $\theta_{\min}^{(i)}$  ( $i=1,2$ ) where the first set is from the DWBA calculation of Madison (Ref. 23) and the second set is from the close-coupling calculations of Fon *et al.* (Ref. 16). The other parameters are from the recommended data of Andersen *et al.* (Ref. 4). The angles are given in degrees.

$E$ (eV)	$\theta_{\max}$ (deg)	$\theta_0$ (deg)	$\theta_{\min}^{(1)}$ (deg)	$\theta_{\min}^{(2)}$ (deg)
30	71	106		
40	58	93	123	107
50	50	83	121	104
60	43	75	118	102
80	37	66	113	98
100	31	60	107	93
150	30	52	99	81
200		45	90	70

TABLE II. The "classical" impact parameter  $b$ 's corresponding to the angles in Table I where  $\langle L_y \rangle$  has maximum, zero, or minimum values and the scaling with respect to the  $vb$  parameter. Both  $b$  and  $v$  are given in atomic units. See text for explanations.

$E$ (eV)	$v$	$b_{\max}$	$b_0$	$b_{\min}^{(1)}$	$vb_{\max}$	$vb_0$	$vb_{\min}^{(1)}$
30	1.48	1.27	0.68		1.88	1.01	
40	1.72	1.22	0.645	0.369	2.10	1.11	0.635
50	1.91	1.17	0.615	0.311	2.22	1.17	0.594
60	2.10	1.15	0.591	0.272	2.41	1.24	0.572
80	2.42	1.02	0.523	0.225	2.46	1.26	0.545
100	2.71	0.981	0.471	0.201	2.65	1.28	0.546
150	3.32	0.654	0.372	0.156	2.17	1.23	0.519
200	3.83		0.328	0.137		1.25	0.526

For the first two angles we adopt the values suggested by Andersen *et al.*,<sup>4</sup> while for  $\theta_{\min}$  we quote the DWBA results of Madison<sup>23</sup> (set 1) and the close-coupling results of Fon *et al.*<sup>16</sup> (set 2) since no accurate experimental data are available. Using Eq. (13) these angles are converted to impact parameters. The corresponding impact parameters  $b$  and the scaling parameter  $vb$  are listed in Table II. We note that both  $vb_0$  and  $vb_{\min}$  are almost constant in the energy region from 30 to about 200 eV except at the lower-energy end. In Fig. 2 we show the plots of  $L_y$  against the scaling parameter  $vb$  for electron-impact excitation on helium at 60 and 150 eV using the results for Madison<sup>23</sup> (which differ somewhat from the recommended values of Andersen *et al.*<sup>4</sup>). It is clear that the two curves of  $L_y$  are very similar. The absolute values of  $L_y$  at the maximum and minimum differ somewhat. The difference implies that the oscillatory structure is most likely due to the oscillation in  $\sin\chi$ , while the absolute value of  $L_y$  is modified by the  $\lambda$ -dependence part [see Eq. (7a)]. The deviations at large  $vb$  (small scattering angles) can partly be due to the unscreened Coulomb potential used in the calculation of impact parameters. From Table II we note that  $b_{\max}$  is greater than 1 a.u. for scattering energies less than 100 eV and thus some screening should be considered in calculating  $b$  from  $\theta$ .

Another relation equivalent to the  $vb$  scaling for electron-impact excitation of hydrogenic ions along the

isoelectronic sequence has been found in Ref. 21. It is noted from Eq. (13) that if the energy  $E$  is expressed in units of the binding energy of the target ion,  $E = E_0 Z^2$ , then

$$b = \frac{Z}{2Z^2 E_0} \cot \frac{\theta}{2} = \frac{1}{2ZE_0} \cot \frac{\theta}{2}. \quad (14)$$

Since  $v$  is scaled linearly with  $Z$ , the scaling of  $vb = \text{const}$  is the same as  $\theta = \text{const}$ , i.e., independent of  $Z$ . In other words, if the collision energy is scaled in  $Z^2$  where  $Z$  is the charge of the hydrogenic ion, then  $L_y$  is a universal function of  $\theta$ , independent of  $Z$ . This is shown in Fig. 3 where the near-universal curves of  $L_y$  calculated using the Coulomb-Born approximation are displayed.

At this time we do not have a fully satisfactory explanation of the scaling relation. The fact that the impact parameter enters in the scaling relation provides further support that the trajectory (defined in some quantum average sense) probably plays an important role in the determination of the behavior of  $L_y$ . From the discussion earlier, we note that the behavior of  $L_y$  versus scattering angle  $\theta$  is mostly determined by  $\sin\chi$ , where  $\chi$  is the

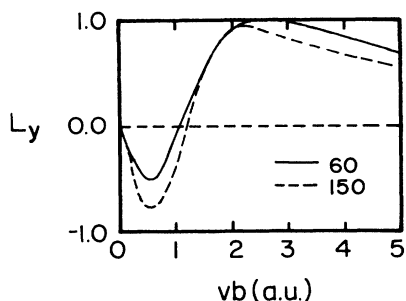


FIG. 2. The scaling of the  $\langle L_y \rangle$  parameter with respect to  $vb$  for electron-impact excitation to helium  $2^1P$  states at 60 and 150 keV. The  $\langle L_y \rangle$  values are obtained from the distorted-wave Born calculations of Madison (Ref. 23).

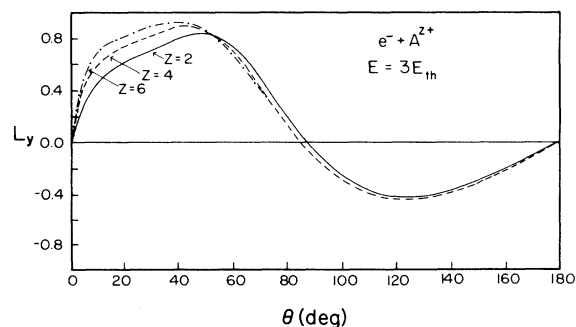


FIG. 3. The scaling of  $\langle L_y \rangle$  for excitation to  $2p$  states of hydrogenic ions (with charge  $Z$ ) for electron-impact energies at  $3E_{\text{th}}$ , where  $E_{\text{th}}$  is the excitation threshold energy which is proportional to  $Z^2$ . Under such a scaling in energies, the  $\langle L_y \rangle$  calculated using the Coulomb-Born approximation is nearly a universal curve as a function of scattering angles (data from Ref. 21).

phase difference of the  $2p_1$  and  $2p_0$  (with respect to the collision frame) amplitudes. According to the eikonal theory, the phase of the scattering amplitude is given by  $(i/v) \int V(r) dz$  where  $r^2 = b^2 + z^2$ . Since  $V(r)$  is approximately given by the Coulomb potential  $1/r$ , the integration over  $dz$  gives a phase that is proportional to  $i/(vb)$ . This would explain qualitatively the origin of the scaling of the phase difference  $\chi$ . No actual calculations have been carried out according to this method yet. Confirmation of this speculation may have to await for eikonal-type calculations.

The simple scaling law observed for excitation to  $2^1P$  states of helium and to  $2p$  states of hydrogenic ions did not apply to the excitation to  $2^3P$  states of helium. Recall that the *calculated* shape of  $L_y$  for the excitation to  $2^3P$  of helium by electron impact is quite similar to that for the excitation to  $2^1P$  states. We have checked the values of  $vb_0$  at the angles where  $L_y$  vanishes using the results from the first-order many-body perturbation calculation. From Table III we note that there is no similar scaling relation. Experimental data<sup>24-26</sup> for the  $L_y$  of excitations to  $2^3P$  and  $3^3P$  states are still quite scarce (experiments are usually carried out for the  $3^3P$  state because the  $2^3P$  state is metastable) and are limited to small angles only. It is not clear how good the theoretical results are. Further discussion of scaling has to wait until more experimental data become available.

### C. Orientation parameters for direct $2p$ and $3p$ excitations of helium by protons and antiprotons

In order to relate the sign of  $L_y$  to trajectory effects, we calculate the orientation parameters for impact excitations of  $2^1P$  and  $3^1P$  states of helium by protons and antiprotons. The calculations were carried out in the intermediate-energy region using a one-center atomic-orbital expansion method where electron capture (by protons) is neglected. Before presenting our results, let us first address the propensity rule for excitation processes discussed by Andersen and Nielsen<sup>27</sup> where they studied the orientation of atomic excited states by atom impact. For direct  $s \rightarrow p$  excitations in the intermediate-energy region,  $L_y$  was shown to be close to  $-1$  according to the propensity rule. This rule can be understood using a three-state, one-center atomic-orbital expansion model, by including the  $s$  state and the two  $p$  states. By using the

TABLE III. Scattering angle  $\theta$  where  $\langle L_y \rangle$  vanishes for electron-impact excitation to  $\text{He}(2^3P)$  states and the corresponding impact parameters  $b_0$  [calculated from Eq. (13) with  $Z=2$ ]. This table shows that the scaling with respect to  $vb_0$  does not work well. Atomic units are used for  $v$  and  $b$ . Data taken from Ref. 6.

$E$ (eV)	$v$	$\theta_0$ (deg)	$b_0$	$vb_0$
30	1.48	100	0.76	1.125
60	2.10	105	0.35	0.731
200	3.83	86	0.15	0.559
500	6.06	68	0.08	0.491

natural frame  $x'y'z'$ , and with the quantization axis chosen to be along  $z'$ , it was shown by Andersen and Nielsen that in the distortion approximation the transition amplitudes for exciting the  $m' = -1$  and  $m' = +1$  states are

$$a_{-1}(+\infty) = -\frac{i}{v} \int_{-\infty}^{+\infty} F(R) \exp \left[ i \left( \frac{\Delta E x'}{v} - \phi \right) \right] dx', \quad (15a)$$

$$a_{+1}(+\infty) = \frac{i}{v} \int_{-\infty}^{+\infty} F(R) \exp \left[ i \left( \frac{\Delta E x'}{v} + \phi \right) \right] dx', \quad (15b)$$

respectively. In the equations above,  $R$  is the internuclear separation  $x' = vt$ ,  $F(R)$  is the projectile and target electron interaction,  $\phi = \phi(R)$  is the rotational angle of the internuclear axis which is positive for repulsive potential and negative for attractive potential, and  $\Delta E$  is approximately the excitation energy between the  $s$  and  $p$  states. For excitation processes where  $\Delta E$  is positive, we note that the phase  $\Delta E x'/v - \phi$  in (15a) tends to vanish for a repulsive potential where  $\phi$  is positive. Using the stationary phase argument, we note that the amplitude in Eq. (15a) is maximum at  $v_M$  when

$$\frac{\Delta E a}{v_M} = \pi. \quad (16)$$

In this equation  $a$  is the range of the interaction; it is the Massey criterion—the condition for determining where the excitation cross section is maximum. When this condition is satisfied, we note that the phase of (15b) goes through  $2\pi$  and thus the amplitude for  $m' = +1$  is much smaller. Thus in the intermediate-energy region, one expects that the  $m' = -1$  state is populated predominantly and thus  $L_y$  tends to  $-1.0$  (recall that in the natural frame  $L_y$  is given by the difference between the  $m' = 1$  and  $m' = -1$  probabilities). This argument further implies that  $L_y$  is not very sensitive to the details of the collision dynamics. However, the effective attractive or repulsive potential is essential. If the interaction is attractive, then the rotational angle changes by  $-\pi$  at the end of the collision. In this case, the  $m' = +1$  component will have large scattering amplitudes and the resulting  $L_y$  will be close to  $+1$ . [Equations (15) also imply that the sign of  $L_y$  will be reversed for deexcitation processes where  $\Delta E$  is negative.]

In Fig. 4 we show the calculated  $L_y$  versus impact parameters for proton-impact excitations of helium to  $2^1P$  and  $3^1P$  states at two energies. The excitation probabilities are also shown. We note that the calculated  $L_y$  is in agreement with the propensity rule for  $s \rightarrow p$  excitations. As a function of impact parameters,  $L_y$  is quite close to  $-1$  for proton impact on helium where the effective interaction is repulsive.

In Fig. 5 we show similar plots for antiproton-impact excitations of helium to  $2^1P$  and  $3^1P$  states. In this case, the effective interaction is attractive and the calculated  $L_y$  is very close to  $+1$ , except at very small impact pa-

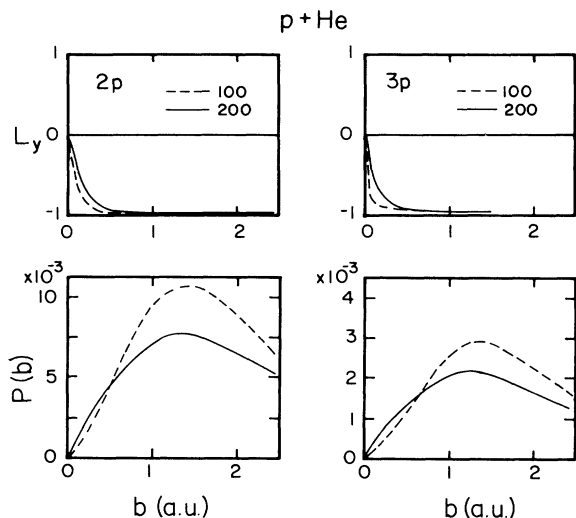


FIG. 4. The  $\langle L_y \rangle$  and excitation probabilities vs impact parameters for excitation to  $2^1P$  and  $3^3P$  states of helium by proton impact at 100 and 200 keV calculated using a one-center atomic-orbital close-coupling expansion method.

rameters. This result is consistent with the propensity rule for an attractive potential. Note that the calculations were carried out using one-center atomic-orbital expansion with a large basis set, including  $s$ -,  $p$ -, and  $d$ -type bound states, and pseudostates which were used to represent continuum orbitals. We have also checked the results using a much smaller basis set, and the resulting values of  $L_y$  are essentially the same. This indicates that the orientation parameter is not very sensitive to the collision dynamics for excitations to  $2^1P$  and  $3^1P$  states in the intermediate-energy region, contrary to the general conception that such measurements always provide more detailed information about the collision dynamics. We remark that we used an independent-electron approximation in the calculation. The helium atom was represented by a model potential which gives the correct binding energies for the ground state and the first few excited states. Such a model has been shown to be quite adequate in many other collision systems.

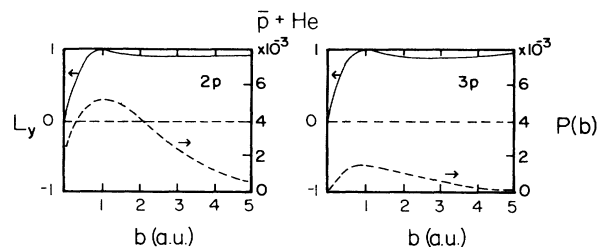


FIG. 5. Same as Fig. 4 but for antiproton-impact excitation on helium at 400 keV. Note that the probabilities are referred to the scale to the right.

#### D. Orientation parameters for excitation and capture to $2p$ and $3p$ states in proton-hydrogen collisions

We next examine the orientation parameters for excitation and electron capture to  $2p$  and  $3p$  states in proton-hydrogen-atom collisions. In Fig. 6 we show the excitation probabilities and  $L_y$  at 50- and 100-keV collision energies and in Fig. 7 similar plots for capture to  $2p$  and  $3p$  states at 35, 50, and 100 keV.

In Fig. 6 we note that excitations to  $2p$  and  $3p$  states occur over a large range of impact parameters and within this range the orientation parameters are very close to  $-1$ , in consistence with the propensity rule. For electron-transfer processes (see Fig. 7), the calculated orientations are different. The  $L_y$  is very small and mostly negative at small impact parameters, reaching a maximum positive value quite close to 1.0 before it drops to negative values at large impact parameters. As the collision energy increases, the impact parameters where  $L_y$  peaks and where  $L_y$  vanishes move to smaller values, but otherwise the general shape does not vary much. [We did not find a similar  $bv$  scaling law (see III B).] We further note that the  $L_y$  for capture to  $2p$  and  $3p$  states are very similar at each given energy.

The results shown above were carried out using a two-center atomic-orbital expansion method with 22 atomic states including some pseudostates on each center. Such calculations have been shown to give accurate total cross sections to each inelastic channel<sup>19-22</sup> and we expect that the reported results for  $L_y$  are quite reliable.

The apparent general behavior of  $L_y$  for capture to  $2p$  states shown in Fig. 7 raises an immediate question as to whether the trend is general. We thus check whether similar dependence can be seen in other rearrangement processes.

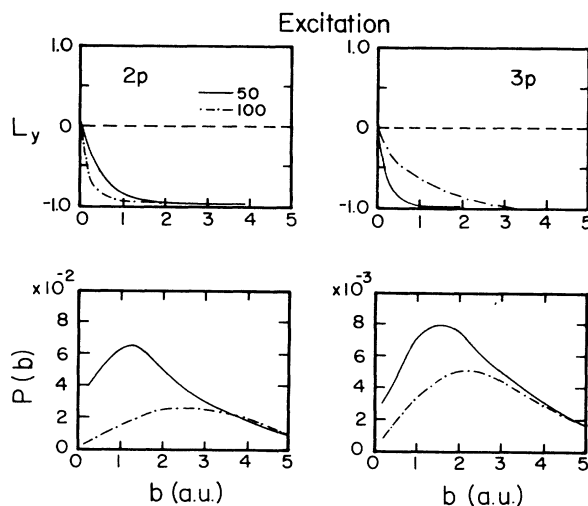


FIG. 6. The excitation probabilities and  $\langle L_y \rangle$  vs impact parameters for excitations to  $2p$  and  $3p$  states in proton-hydrogen-atom collisions at 50 and 100 keV.



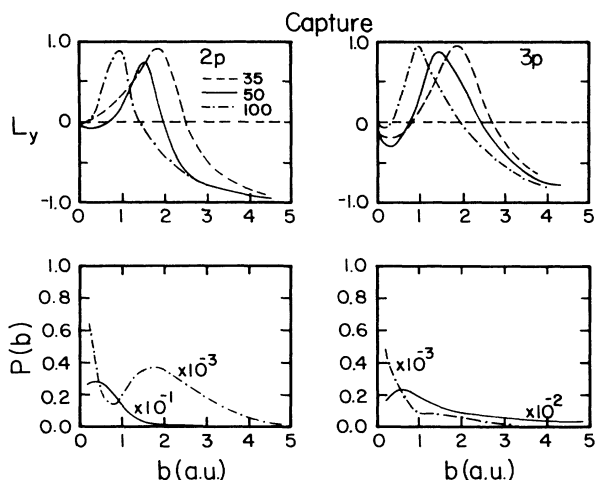


FIG. 7. The electron capture probabilities and  $\langle L_y \rangle$  vs impact parameters for electron capture to  $2p$  and  $3p$  states in proton-hydrogen collisions at 35, 50, and 100 keV.

#### E. Orientation of positronium $2p$ states in positron-hydrogen collisions

In Fig. 8 we show the orientation of positronium  $2p$  states formed in the collision between positrons and hydrogen atoms using the scattering amplitudes obtained from the distorted-wave Born approximation.<sup>28</sup> The results at 40 and 60 eV are shown.<sup>29</sup> We note that  $L_y$  is very insensitive to the incident energy. The value of  $L_y$  is negative at both small and large angles, but positive at intermediate angles. Its shape is similar to those shown for capture to  $2p$  states in proton-hydrogen collisions at comparable velocities.

We remark that the validity of the distorted-wave Born calculation for the formation of  $2p$  positronium states has

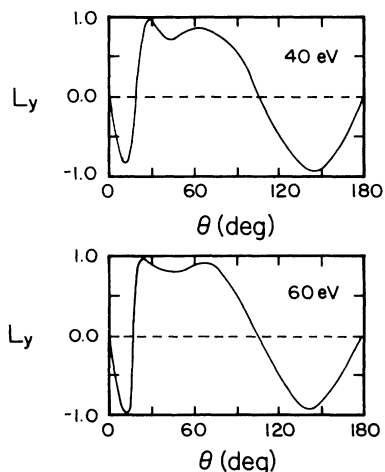


FIG. 8. The  $\langle L_y \rangle$  of the positronium  $2p$  states formed in positron-hydrogen-atom collisions at 40 and 60 eV calculated using the distorted-wave approximation.

not been confirmed either by other elaborate calculations and/or experiments and the reliability of the calculated  $L_y$  has not been tested. On the other hand, the coupled-channel calculations carried out for proton-hydrogen collisions have been well tested<sup>20-23</sup> and we expect that the results for  $L_y$  will be proven correct in the future. The similarity in the shape of  $L_y$  in the  $2p$  states for positron and proton collisions with hydrogen atoms *probably* indicates that  $L_y$  is not very sensitive to the detailed theory used in the calculation so long as the distortion effect is included. More calculations or experiments have to be carried out before one can conclude whether the general shape of  $L_y$  seen here is an indication of a "propensity rule" for rearrangement collisions to  $2p$  states.

#### F. The orientation parameters for $3d$ states

The simple results presented above seem to indicate that there is a relation between the attractive and repulsive effective interaction between the collision partners and the shape (and the sign) of  $L_y$ . The question is whether this is true for excitation to other states. We thus examine the  $L_y$  for  $3d$  states. If the scattering amplitudes are expressed in the collision frame, from Eq. (8a) one notes that there are two terms contributing to  $L_y$ , one from the  $3d_0$  and  $3d_1$  amplitudes, and the other from the  $3d_1$  and  $3d_2$  amplitudes. If expressed in the natural frame,  $L_y$  becomes simply the difference in the probabilities of populating the  $m'=2$  and  $m'=-2$  states [see Eq. 8(b)].

In Fig. 9 we show the calculated  $L_y$  for excitation and capture to  $3d$  states in proton-hydrogen collisions at 20 and 35 keV. The calculations were carried out at lower

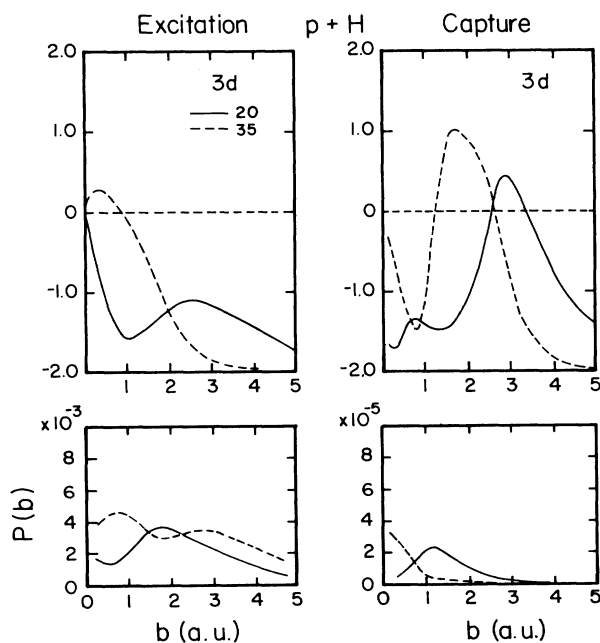


FIG. 9. The excitation probabilities and  $\langle L_y \rangle$  for excitation and electron capture to  $3d$  states in proton-hydrogen collisions at 20 and 35 keV.

energies so that the  $3d$  cross sections are not too small. First we note that the  $L_y$  for excitations is mostly negative and approaches  $-2.0$  at large impact parameters, in accordance with the propensity rule for  $d$  states studied by Nielsen and Andersen<sup>27</sup> in a one-center atomic-orbital expansion model. Interpretations based on the distortion approximation similar to those used for  $s$ - $p$  transitions can be applied to understand the propensity rule for  $s$ - $d$  transitions. The small kink for the 20-keV results at  $b=2-4$  a.u. reflects the structure usually seen for low-energy collisions.

In Fig. 9 we also show the  $L_y$  for capture to  $3d$  states at 20 and 35 keV. The shape of each curve is quite similar to those shown for capture to  $2p$  and  $3p$  states in that  $L_y$  is negative at both large and small impact parameters, but positive in the intermediate range. The probabilities for capture to  $3d$  states are also shown. We note that capture to  $3d$  states occurs at increasingly small impact parameters as the collision energy increases.

The angular dependence of  $L_y$  for electron-impact excitations to  $3d$  states is still rather confusing. New experimental data carried out at 40 eV at three angles<sup>30</sup> ( $\theta < 60^\circ$ ) indicated that  $L_y$  is negative at small angles, contrary to the positive  $L_y$  for excitations to  $2p$  states. Theoretical calculations are very inconclusive. The DWBA calculations<sup>31</sup> show that the results are very sensitive to the distortion potentials used. Calculations based on the first-order many-body perturbation theory<sup>32</sup> and those from the ten-state eikonal approximation<sup>33,34</sup> do not agree with each other at this energy nor at higher energies. The eikonal calculation indicates that the shape of  $L_y$  changes as the collision energy increases. In view of the lack of experiments and a general consensus of the behavior of  $L_y$  for  $3d$  states, we cannot draw any conclusions at this time. Before concluding this section, we also point out that the Coulomb-Born calculations<sup>21</sup> for electron- and positron-impact excitations of hydrogenic ions to  $3d$  states predict that the angular dependence of  $L_y$  does not display any simple general behavior.

#### IV. THE ALIGNMENT ANGLE $\gamma$

We have also examined the alignment angle  $\gamma$ , as defined in Eq. (7b) for  $2p$  states. Within the first Born approximation, the major axis of the charge cloud is along the direction of the momentum transfer  $\mathbf{q} = \mathbf{k}_i - \mathbf{k}_f$ , and the angle  $\gamma$  is given by

$$\tan\gamma = \frac{\sin\theta}{\cos\theta - x}, \quad (17a)$$

where

$$x = \frac{k_i}{k_f} = \left[ \frac{E}{E - \Delta E} \right]^{1/2}. \quad (17b)$$

From (17a) and (17b) we see immediately that  $\gamma$  is negative for excitation processes in the Born approximation. In fact, for heavy-particle collisions,  $\Delta E$  is much smaller than  $E$ , thus Eq. (17a) is given by

$$\tan\gamma = -\cot(\theta/2). \quad (18a)$$

If we assume a Coulomb trajectory, then

$$b = \frac{13.6}{1000[E(\text{keV})]} \cot(\theta/2) \quad (18b)$$

and the alignment angle  $\gamma$  expressed in terms of  $b$  is

$$\tan\gamma = -\frac{1000[E(\text{keV})]}{13.6} b, \quad (18c)$$

where  $b$  is given in atomic units. Therefore the alignment angle is close to  $-90^\circ$  for heavy-particle collisions in the Born approximation.

In Fig. 10 we show the angles  $\gamma$  for excitation and capture to  $2p$  states for proton-hydrogen-atom collisions at 50 and 100 keV. The results show that the angle  $\gamma$  for excitation to  $2p$  at 50 keV still deviates significantly from the prediction of the Born approximation. At 100 keV, the deviation from the prediction of the Born approximation becomes smaller, but significant difference still occurs for  $b < 1$  a.u.

The angle  $\gamma$  for capture to  $2p$  states is much more difficult to interpret. At the two energies shown, there is no apparent simple relation. In fact, the structures for  $\gamma$  in general are more complicated and no simple systematics have emerged in all the studies so far, i.e., either by electron- and positron-impact, or by proton- and atom-impact excitations.

The complicated angular or impact parameter dependence of  $\gamma$  makes the systematic study of this parameter less attractive. To see if there is simpler dependence of the  $\lambda$  and  $\chi$  parameters with impact parameters, we show

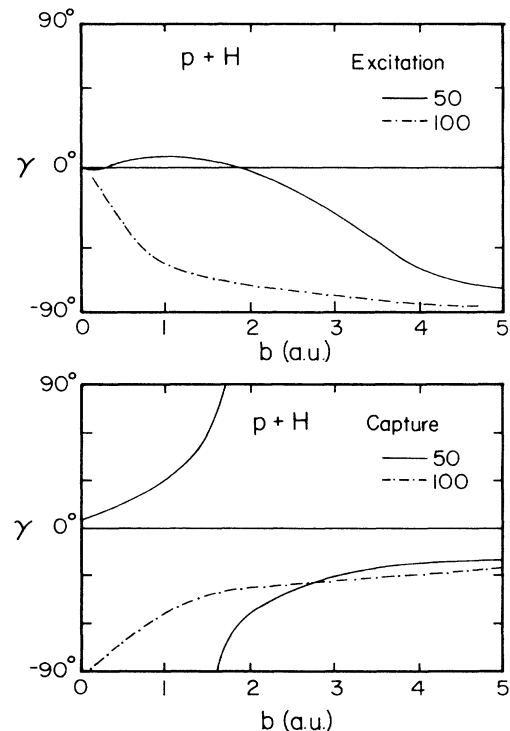


FIG. 10. The alignment angles  $\gamma$  for excitation and capture to  $2p$  states in proton-hydrogen collisions at 50 and 100 keV.

in Fig. 11 these two parameters at 35, 50, and 100 keV for the excitation and capture to  $2p$  states. The results do not show any simple trends either except that the phase difference  $\chi$  tends to approach  $90^\circ$  for excitations at large impact parameters. Since there is no indication of simple systematics, we decide not to pursue this matter further. It appears that one has to treat each collision system at each energy separately.

## V. SUMMARY AND CONCLUSIONS

In this article we analyzed the general behavior of the orientation parameter  $\langle L_y \rangle$  and alignment angle  $\gamma$  for the atomic excited states in the collision of helium or hydrogen atoms with electrons, positrons, protons, and antiprotons. For electron and positron impact, we rely on results in the literature and from private communications. For proton and antiproton impact, we obtain results from the coupled-channel calculations in the impact parameter approximation.

For excitation to  $2p$  states (for hydrogen target) or to  $2^1P$  states (for helium target), we showed that the sign of  $\langle L_y \rangle$  is consistent with the classical model except for electron-impact excitations at large angles. According to this model,  $\langle L_y \rangle$  is positive if the interaction potential between the projectile and the target atom is attractive and is negative if the interaction potential is repulsive. Thus theoretical and available experimental results indicate that  $\langle L_y \rangle$  is positive for electron- and antiproton-impact excitations and negative for positron- and proton-impact excitations. The negative  $\langle L_y \rangle$  for electron-impact excitations at large angles cannot be interpreted classically, but could be attributed to the strong attractive potential which results in large phase shifts.

We have identified that the angular dependence of  $\langle L_y \rangle$  for electron-impact excitations to  $2p$  states is mostly due to  $\sin\chi$  where  $\chi$  is the phase angle between the  $2p_1$  and  $2p_0$  states in the collision frame. We have found a semiempirical scaling law for  $\langle L_y \rangle$  in terms of effective impact parameters at different energies. The origin of the scaling was attributed approximately to the energy dependence of the eikonal phase.

We have studied the validity of the propensity rule for direct excitation processes. It was found that for excitations by protons,  $\langle L_y \rangle$  is mostly negative and close to  $-1$ , and for excitations by antiprotons,  $\langle L_y \rangle$  is mostly positive and close to  $+1$ , in accordance with the propensity rule of Andersen and Nielsen.

We have examined the  $\langle L_y \rangle$  for  $2p$  states formed in rearrangement collisions. For positron-impact collisions, we have found that  $\langle L_y \rangle$  is negative at small and large angles and positive at intermediate angles. Similarly,  $\langle L_y \rangle$  was found to be negative at small and large impact parameters and positive at intermediate impact parameters. It appears that such angular (or impact parameter) dependences are quite general and the results are insensitive to scattering energies. Future experiments and/or theoretical calculations should address the validity of this dependence and its possible simple interpretations.

We have also examined the orientation parameters for

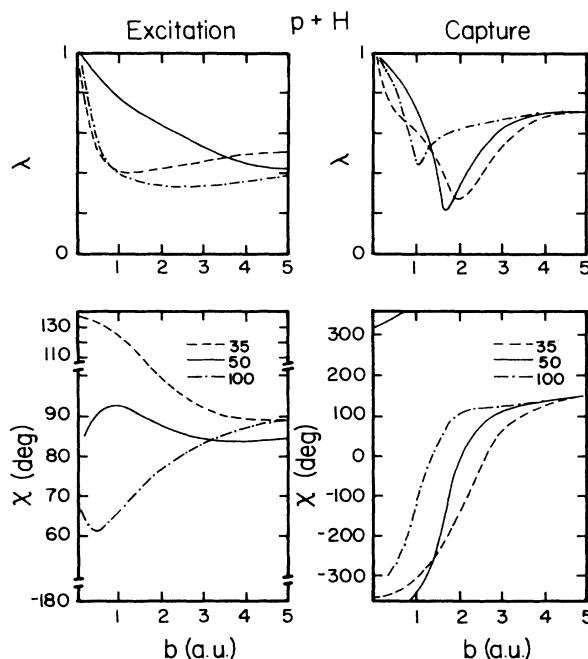


FIG. 11. The  $\lambda$  and  $\chi$  parameters for excitation and capture to  $2p$  states in proton-hydrogen collisions at 35, 50, and 100 keV.

excitation and capture to  $3d$  states in proton-hydrogen collisions. For the excitation process, it was found that the propensity rule applies and that  $\langle L_y \rangle$  is very close to  $-2.0$ . For the electron capture process,  $\langle L_y \rangle$  is negative at both large and small impact parameters but positive in between, similar to that for electron capture to  $2p$  states. For electron-impact excitation to  $3d$  states, the results for  $\langle L_y \rangle$  are still very inconclusive, both experimentally and theoretically. It is not clear that there will be any simple systematics, not to mention whether eventually the results can be related to the interaction potentials.

A similar attempt was made to address the alignment angles  $\gamma$  for excitation and capture to  $2p$  states. We found that there is no indication of simple systematics for this parameter and it appears that this angle varies in a relatively complicated manner with energies, thus defying simple interpretations. Therefore no effort was made to document the impact parameter dependence of  $\gamma$  except for the few examples explored. We have also explored the energy dependence of the  $\lambda$  and  $\chi$  parameters and no simple relations were found. We thus tentatively conclude that unlike the  $\langle L_y \rangle$  parameter, these other parameters reflect individual collision systems and collision energies.

We have not addressed the more complicated target atoms to explore the effect of the nodal structure in the initial-state wave functions on the angular dependence of  $\langle L_y \rangle$  and other parameters. Similarly, we have not yet examined similar parameters for collisions with polarized excited target atoms which are under investigation exper-

imentally.

We conclude this paper by pointing out that for hydrogenic excited states one can examine the coherence among the hydrogenic  $nl$  states for each  $n$  manifold. One can explore the difference in the dipole moments and other parameters of hydrogenic excited states in collisions with electrons, positrons, protons, and antiprotons as well. Such a study, although not complete, has been carried out earlier.<sup>11</sup>

#### ACKNOWLEDGMENTS

This work was supported in part by the U.S. Department of Energy, Office of Basic Energy Sciences, Division of Chemical Sciences. We thank Dr. D. H. Madison and Dr. S. N. Nahar for sending us some unpublished scattering amplitudes for the analysis reported here and Dr. U. Fano and Dr. D. H. Madison for comments on the original manuscript.

<sup>1</sup>U. Fano and J. H. Macek, *Rev. Mod. Phys.* **45**, 553 (1973).

<sup>2</sup>K. Blum, *Density Matrix, Theory and Applications* (Plenum, New York, 1981).

<sup>3</sup>J. Macek, in *Fundamental Processes in Energetic Atomic Collisions*, Vol. 103 of *NATO Advanced Study Institute, Series B: Physics*, edited by H. O. Lutz (Plenum, New York, 1983).

<sup>4</sup>N. Andersen, J. Gallagher, and I. V. Hertel, *Phys. Rep.* **165**, 1 (1988).

<sup>5</sup>D. H. Madison and K. H. Winters, *J. Phys. B* **16**, 4437 (1983), and references therein.

<sup>6</sup>G. Csanak and D. C. Cartwright, *Phys. Rev. A* **34**, 93 (1986); D. C. Cartwright and G. Csanak, *J. Phys. B* **19**, L485 (1986).

<sup>7</sup>N. C. Steph and D. E. Golden, *Phys. Rev. A* **23**, 647 (1980).

<sup>8</sup>D. H. Madison, G. Csanak, and D. C. Cartwright, *J. Phys. B* **19**, 3361 (1986).

<sup>9</sup>R. Hippler, M. Faust, R. Wolf, H. Kleinpoppen, and H. O. Lutz, *Phys. Rev. A* **36**, 4644 (1987); see the review of N. Andersen, J. Gallagher, and I. V. Hertel, *Phys. Rep.* (to be published).

<sup>10</sup>J. Burgdörfer, *Z. Phys. A* **309**, 285 (1983).

<sup>11</sup>A. Jain, C. D. Lin, and W. Fritsch, *J. Phys. B* **21**, 1545 (1987), and references therein.

<sup>12</sup>C. C. Havener, N. Rouze, W. Westerveld, and J. S. Risley, *Phys. Rev. A* **33**, 276 (1986).

<sup>13</sup>M. Eminyan, K. B. MacAdam, J. Slevin, and H. Kleinpoppen, *J. Phys. B* **7**, 1519 (1974).

<sup>14</sup>M. C. Standage and H. Kleinpoppen, *Phys. Rev. Lett.* **36**, 577 (1976).

<sup>15</sup>N. Andersen, T. Andersen, J. S. Dahler, S. E. Nielsen, G. Nienhuis, and K. Refsgaard, *J. Phys. B* **16**, 817 (1983).

<sup>16</sup>W. C. Fon, K. A. Berrington, and A. E. Kingston, *J. Phys. B* **13**, 2309 (1980).

<sup>17</sup>E. J. Mansky and M. R. Flannery, *J. Phys. B* **20**, L235 (1987).

<sup>18</sup>D. R. Bates, *Proc. R. Soc. London, Ser. A* **274**, 294 (1958).

<sup>19</sup>W. Fritsch and C. D. Lin, *Phys. Rev. A* **26**, 762 (1982).

<sup>20</sup>R. Shingal and B. H. Bransden, *J. Phys. B* **20**, 4815 (1987).

<sup>21</sup>A. Jain, C. D. Lin, and W. Fritsch, *J. Phys. B* **21**, 1545 (1988).

<sup>22</sup>W. Fritsch and C. D. Lin, *Phys. Rep.* (to be published).

<sup>23</sup>D. H. Madison (private communication).

<sup>24</sup>J. P. M. Beijers, S. J. Doornenbal, J. van Eck, and H. G. M. Heideman, *J. Phys. B* **19**, L837 (1987).

<sup>25</sup>I. Humphrey, J. F. Williams, and E. L. Heck, *J. Phys. B* **20**, 367 (1987).

<sup>26</sup>H. A. Slim, H. J. Beyer, El. A. El-Sheikh, and H. Kleinpoppen, *J. Phys. B* **18**, 4454 (1987).

<sup>27</sup>N. Andersen and S. E. Nielsen, *Z. Phys. D* **5**, 309 (1987).

<sup>28</sup>R. Shakeshaft and J. M. Wadehra, *Phys. Rev. A* **22**, 968 (1980).

<sup>29</sup>Scattering amplitudes provided by S. N. Nahar (private communication).

<sup>30</sup>S. E. Nielsen and N. Andersen, *Z. Phys. D* **5**, 321 (1987).

<sup>31</sup>J. P. M. Beijers, S. J. Doornenbal, J. van Eck, and H. G. M. Heideman, *J. Phys. B* **18**, 4135 (1987).

<sup>32</sup>K. Bartschat and D. H. Madison, *J. Phys. B* **21**, 153 (1988).

<sup>33</sup>D. C. Cartwright and G. Csanak, *J. Phys. B* **20**, L583 (1987).

<sup>34</sup>E. J. Mansky and M. A. Flannery, *J. Phys. B* **20**, L235 (1987).